Ressler, A.; Ródenas Rochina, J.; Ivankovic, M.; Ivankovic, H.; Rogina, A.; Ferrer, G. (2018). Injectable chitosan-hydroxyapatite hydrogels promote the osteogenic differentiation of mesenchymal stem cells. Carbohydrate Polymers. 197:469-477. https://doi.org/10.1016/j.carbpol.2018.06.029

# Injectable chitosan-hydroxyapatite hydrogels promote the osteogenic differentiation of mesenchymal stem cells

Antonia Ressler[a;*], Joaquín Ródenas-Rochina[b], Marica Ivanković[a], Hrvoje Ivanković[a], Anamarija Rogina[a], Gloria Gallego Ferrer[b,c]

[a] Faculty of Chemical Engineering and Technology, University of Zagreb, HR-10001 Zagreb, Marulićev trg 19, p.p.177, Croatia

[b] Centre for Biomaterials and Tissue Engineering, Universitat Politècnica de València, Camino de Vera s/n, 46022 Valencia, Spain

[c] Biomedical Research Networking Centre in Bioengineering, Biomaterials and Nanomedicine (CIBER-BBN), Valencia, Spain

*Corresponding author: Antonia Ressler, Faculty of Chemical Engineering and Technology, University of Zagreb, HR-10001 Zagreb, Marulićev trg 19, p.p.177, Croatia, Tel: +385 01 4597 210, e-mail: aressler@fkit.hr

E-mail addresses: aressler@fkit.hr (A. Ressler), jrodenasr@gmail.com (J. Ródenas Rochina), mivank@fkit.hr (M. Ivanković), hivan@fkit.hr (H. Ivanković), arogina@fkit.hr (A. Rogina), ggallego@ter.upv.es (G. Gallego Ferrer).

**Abstract**

Injectable hydrogels have emerged as promising biomaterials for tissue engineering applications. The goal of this study was to evaluate the potential of a pH-responsive chitosan-hydroxyapatite hydrogel to be used as a three-dimensional support for encapsulated mesenchymal stem cells (MSCs) osteogenic differentiation. *In vitro* enzymatic degradation of the hydrogel, during 28 days of incubation, in simulated physiological condiditons, was characterized by swelling measurements, molecular weight determination and SEM analysis of hydrogel microstructure. Osteogenic differentiation of encapsulated MSCs was confirmed by osteogenic Runx2, collagen type I and osteocalcin immunostaining and alkaline phosphatase quantification. The deposition of late osteogenic markers (calcium phosphates) detected by Alizarin red and von Kossa staining indicated an extracellular matrix mineralization.

Keywords: chitosan; differentiation; hydrogel; hydroxyapatite; MSCs; osteogenesis

## 1. Introduction

Over the past decade, injectable hydrogels have emerged as promising biomaterials for tissue engineering applications since they are generally biocompatible, biodegradable and can mimic the extracellular matrix (ECM) architecture. With the fast development of cell-based therapies, there is a growing need to develop injectable hydrogels as cell carriers, potentially avoiding an open surgery procedure and facilitating the use of minimally invasive approaches for material and cell delivery. The hydrogel precursor loaded with cells can be injected into the wound site, and experiences a sol–gel transition *in situ* due to physical or chemical stimuli.

In the past years, many chitosan (Cht) based hydrogels have been developed for biomedical applications, as it is well documented and analyzed in review papers (Liu et al., 2017; Racine, Texier & Auzély-Velty, 2017; Ta, Dass & Dunstan, 2008). A particular focus has been on chitosan hydrogels based on thermosensitive sol−gel transition initiated by glycerophosphate salt at body temperature, invented by Chenite et al. (Chenite, Buschmann, Wang, Chaput, & Kandani, 2001). The ability of chitosan-based hydrogels to support chondrogenic differentiation of human mesenchymal stem cells (hMSCs) has been confirmed (Cho et al., 2004; Dang et al., 2006). By combining chitosan–glycerophosphate with different concentrations of starch, a thermoresponsive hydrogel, that can be used as an injectable vehicle for cell delivery, has been prepared (Sa-Lima, Caridade, Mano, & Reis, 2010). Naderi-Meshkin et al. (Naderi-Meshkin et al., 2014) have developed a chitosan based injectable hydrogel via the combination of chitosan, glycerol phosphate, and hydroxyethyl cellulose. Systematic investigations of the viability, proliferation, and differentiation capacity of encapsulated mesenchymal stem cells in the hydrogel have indicated that the hydrogel has a high potential for cartilage tissue engineering. The study with human adipose-derived stem cells grown on chitosan hydrogel, cross-linked by 0.5% glutaraldehyde, (Debnath et al., 2015)

has revealed that chitosan hydrogel promotes cell proliferation coupled with > 90% cell viability.

Chitosan hydrogels loaded with inorganic particles, such as hydroxyapatite (HAp), which is the inorganic component of bone and constitutes 60 % of native bone ECM, have been prepared to improve mechanical properties and bioactivity of hydrogels. The addition of hydroxyapatite phase into chitosan-based material has indicated better cell and protein adhesion, enhanced cell proliferation and higher osteogenic gene expression (Frohbergh et al., 2012; Peter et al., 2010). Moreover, stem cell culture on chitosan-hydroxyapatite scaffolds modified by growth factors has been proposed as good strategy for bone tissue reconstruction (Liu et al., 2013). In a recent study (Demirtas, Irmak & Gümüşderelioğlu, 2017) a chitosan solution and its composite with nanostructured hydroxyapatite were mixed with cells and bioprinted successfully. It was observed that MC3T3-E1 pre-osteoblast cells within chitosan and chitosan-HA hydrogels had mineralized and differentiated osteogenically after 21 days of culture. It was proven that the presence of hydroxyapatite in chitosan hydrogels improved cell viability, proliferation and osteogenic differentiation.

In our recent study (Rogina et al., 2017b) a novel pH-responsive chitosan-hydroxyapatite hydrogel, physically crosslinked with sodium bicarbonate, that allowed non-cytotoxic fast gelation within 4 min, was prepared, with 30% (w/w) of HAp phase. The *in situ* synthesis of apatite phase has facilitated the physical crosslinking by reducing the acidity of the chitosan solution. Preliminary biological characterization of the hydrogel, performed by MTT test and live-dead assay, indicated good distribution and viability of encapsulated mouse embryonic fibroblasts and good resistance to shear. Based on these results we hypothesized that proposed injectable hydrogel could be a suitable osteoconductive cellular carrier.

*In this* work, as a continuation of previous studies, *in vitro* enzymatic degradation of the hydrogel, during 28 days of incubation, in simulated physiological condiditons, has been analyzed. To evaluate the osteogenic potential of the hydrogel, an extensive biological characterization has been preformed as well, using porcine mesenchymal stem cells. Since our recent studies proved the osteogenic potential of highly porous composite Cht/HAp scaffold, with 30 wt% of *in situ* formed HAp, prepared by precipitation reaction and freeze-gelation method in static and dynamic cell culture conditions (Rogina et al., 2016; Rogina et al., 2017a) in this work, we used the Cht/HAp scaffold, as a control. We hypothesized that the cellular response to chemically identical biomaterials may depend on the way the cells were incorporated in biomaterial. Therefore, two methods were applied: (1) MSCs were encapsulated during chitosan-hydroxyapatite hydrogel formation and (2) cells were seeded onto prefabricated porous chitosan-hydroxyapatite scaffold, and the results of biological characterization were compared.

## 2. Materials and methods

### 2.1. Materials

Chitosan (Cht, $M_w$ = 100 – 300 kg/mol, deacetylation degree of 0.95 – 0.98, Acros Organics; sterilised with 96% of ethanol), calcium carbonate ($CaCO_3$, calcite; TTT; sterilised by autoclave), urea phosphate ($(NH_2)_2CO–H_3PO_4$); Aldrich Chemistry; sterilised using 0.22 µm filter), acetic acid (99.5 %, Sigma Aldrich; sterilised using 0.22 µm filter), sodium bicarbonate ($NaHCO_3$, Gram-Mol; sterilised using 0.22 µm filter), sodium hydroxide (NaOH, Gram-Mol) and ethanol (EtOH, 96% Kefo) were all of analytical grade. Lysozyme (from hen egg white, ≥ 54 000 U/mg protein) in the form of powder was purchased from Sigma-Aldrich.

123 2.2. Synthesis of pH-responsive Cht/HAp hydrogel and scaffold

124

125 Based on our previous study (Rogina et al., 2015) chitosan-hydroxyapatite suspension
126 was prepared by *in situ* wet precipitation method. Briefly, 1.2 wt% of chitosan (Cht) solution
127 was prepared in 0.36 wt% acetic acid (HAc). Then, calcite ($CaCO_3$) and urea phosphate
128 ($(NH_2)_2CO–H_3PO_4$) were added into Cht solution with Ca/P ratio of 1.67 to obtain 30 wt% of
129 hydroxyapatite in final composite. This HAp content was selected based on our previous
130 studies on chitosan composite scaffolds (Rogina et al., 2015; Rogina et al., 2016; Rogina et
131 al., 2017a) where it resulted optimal in terms of mechanical and biological response as
132 stimulates osteogenesis.
133 The mixture was stirred 4 days at 50 °C. After 4 days of reaction, the Cht/HAp suspension
134 was cooled down naturally to ambient temperature and used for preparation of pH-responsive
135 hydrogel (1) and control material (2).
136 (1) The pH-responsive, Cht/HAp system was prepared using 0.067 mg/L solution of sodium
137 bicarbonate prepared in basal α-MEM (minimum essential medium), as described previously
138 (Rogina et al., 2017b). After cooling down the Cht/HAp suspension and $NaHCO_3$/α-MEM
139 solution to 10 °C using ice bath, components were mixed together for 10 sec by stirring at
140 1700 rpm. Homogenized suspension was then incubated at 37 °C to initiate physical
141 crosslinking of Cht/HAp hydrogel.
142 (2) The Cht/HAp scaffolds prepared by thermally induced phase separation and extraction
143 (Rogina et al., 2015) were used as control materials. Briefly, Cht/HAp suspension was frozen
144 over night at -22 °C and immersed in NaOH/EtOH (1:1 of volume portion) solution for 12 h
145 at -22 °C. Then, samples were immersed in ethanol for 12 h at -22 °C and finally dehydrated
146 in ethanol for 24 h, at ambient temperature.

147 2.3. *In vitro* enzymatic degradation

The degradation behaviour of Cht/HAp crosslinked hydrogel was studied at two different concentrations of lysozyme (1.5 µg/mL corresponding to an activity of 82 U/mL and 500 µg/mL corresponding to an activity of 27 300 U/mL) under static physiological conditions (phosphate buffer saline solution, PBS) on five replicas. Crosslinked hydrogels (*n* = 5, 500 µL) were incubated in 5 mL of PBS containing lysozyme at 37 °C during 28 days. Freshly prepared degradation medium was changed every third day to maintain the activity of lysozyme and to mimic physiological conditions *in vivo* (Porstmann et al., 1989). The Cht/HAp hydrogels were also incubated in phosphate buffer saline solution without containing lysozyme. At defined time points, the degradation medium was carefully removed in order to determine the weight of swollen hydrogel samples ($W_s$). Then, samples were lyophilised ($W_d$) and swelling ratio was calculated according to equation 1:

$$Swelling\ ratio(\%) = \frac{W_s - W_d}{W_d} \times 100 \quad (1)$$

The degradation of hydrogels was determined as the ratio of remaining hydrogel weight ($W_d$) and initial weight of the sample ($W_{d0}$) before enzymatic degradation (Eq. 2).

$$Dry\ weight\ remaining\ ratio(\%) = \frac{W_d}{W_{d0}} \times 100 \quad (2)$$

The influence of degradation medium on hydrogels' microstructure was analysed by scanning electron microscopy (SEM). Dried degraded samples were coated with plasma of gold and palladium for 90 s. The microscopic imaging was carried out by the electron microscope TESCAN Vega3SEM Easyprobe at electron beam energy of 15 keV.

172 2.4. Gel permeation chromatography

173 The distribution of molecular weight of Cht/HAp hydrogels during enzymatic
174 degradation was analysed by Gel Permeation Chromatography (GPC), at 35 °C, with a Waters
175 Breeze GPC system and a 1525 Binary HPLC pump (Waters Corporation, Milford, MA)
176 equipped with a 2414 refractive index detector and four serial columns of water
177 (Ultrahydrogel 7.8 mm ID X 30 cm). The degraded hydrogel samples were dissolved in acetic
178 buffer ($CH_3COOH$ 0.5 M/$CH_3COONa$ 0.2 M, pH = 4.5) used as a mobile phase at a flow rate
179 of 0.5 mL/min and 20 µL injection volume, as previously described by Gámiz-González et al.
180 (Gámiz-González et al., 2015).

181

182 2.5. Cell encapsulation/seeding

183 Porcine mesenchymal stem cells from bone marrow were obtained, using a modified protocol
184 for human MSCs isolation (Gamiz-Gonzalez et al., 2017; Lennon & Caplan, 2006; Rodenas-
185 Rochina, Kelly, Ribelles & Lebourg, 2016; Thorpe et al., 2008). For expansion, the cells were
186 seeded at $4 \times 10^5$ cells/$cm^2$ in a T75 $cm^2$ culture flask with high glucose Dulbecco's modified
187 Eagle's medium (DMEM), enriched with 10% of FBS, 2% penicillin/streptomycin and 125
188 µg/mL amphotericin B until passage 1. From passage 1 to 3 culture media was supplemented
189 with 5 ng/mL recombinant human fibroblast growth factor- 2 and without amphotericin B.
190 Cells at passage 3 were used for tri-potentiality assessment (Thorpe et al., 2008) and cell
191 culture seeding.

192 For cell encapsulation, the cells were resuspended at a density of $1.4 \times 10^6$ cells/mL in a
193 Cht/HAp/$NaHCO_3$ solution, with pH of 7.01 and at 10 ºC suitable for cell survival, as
194 described in our previous study (Rogina, et al.; 2017b).

The cell/hydrogel system was quickly seeded on 24-well plates, 200 µL per well, and incubated in humidified atmosphere at 37 °C and 5% of $CO_2$ for 4 min to induce physical crosslinking. Then, samples were incubated with 2 mL of DMEM medium supplemented with 10% of FBS (fetal bovine serum) and 1% of penicillin/streptomycin in a humidified atmosphere with 5% $CO_2$ at 37 °C for 24 h. After 24 h, basal medium was changed with DMEM supplemented with 10% of FBS, 1% of penicillin/streptomycin, 50 µg/mL of ascorbic acid, 10 mmol/L of $\beta$-glycerophosphate and 1 µmol/L of dexamethasone. The medium was refreshed every third day.

As a control material, Cht/HAp scaffolds were cut into cylindrical shape pieces of 7 mm diameter and 1-2 mm height, sterilized in 96% ethanol and conserved at 4 °C for 24 h. After sterilization, scaffolds were washed 3 times with Dulbecco's modified Eagle's culture medium (DMEM), left in DMEM for 24 h and transported into 24-well plate. Scaffolds were seeded with the same cell density as hydrogels, according to the volume of the scaffold. The cells suspension was put on top of the scaffold and incubated for 15 min to allow cells attachment and migration inside the scaffold. Then cell culture media was added in the same way as for the hydrogels.

## 2.6. Cell Counting

Cell proliferation into Cht/HAp hydrogels and control materials was examined at 1, 7 and 14 days of culture. After cutting three 50 µm slices, of five different replicas, samples were stained with DAPI. Images were taken by confocal fluorescence microscope (Zeiss LSM 780, Axio Observer) in 16-tile mode scanning and the cell nuclei were counted. Average number of cells at different time points is expressed as average value corrected by standard error of the mean (SEM).

## 2.7. Alkaline phosphatase analysis

The activity of alkaline phosphatase (ALP) was measured as the conversion of p-nitrophenylphosphate to p-nitrophenol as the result of the cellular extract activity, using SensoLyte® pNPP Alkaline Phosphatase Assay kit *Colorimetric* (AnaSpec) according to the manufacturer instructions. Samples were gathered at 7 and 14 days. For each time point, three acellular samples were used as blanks. After washing the samples with Dulbecco's phosphate buffered saline (DPBS) and lysis buffer (DPBS 1X with 0.2 % Triton X-100) solution, 200 µL of lysis buffer was added and homogenized with hydrogel. All samples were incubated in ice bath and centrifuged at 4 °C for 7 min to precipitate cellular and material debris. Then, 50 µL of each standard and sample with 50 µL of p-nitrophenylphosphate were placed in 96-well plate in triplicates. The plate was incubated in the dark for 40 min at room temperature. Absorbance was measured at 405 nm using Perkin-Elmer VICTOR3 multi-plate reader. The concentration of the ALP was determined using a standard curve.

## 2.8. Immunofluorescent imaging of cell markers

Differentiation of MSCs at 7 and 14 days was evaluated by different antibodies to confirm the expression of differentiation markers: runt-related transcription factor 2 (Runx2), collagen type I (COLL I) and osteocalcin (OCN). Cultured samples were fixed in 4% of formaldehyde at 4 °C for 1 h and washed with DPBS. Sample slices of Cht/HAp hydrogels with 50 µm of thickness were permeabilized with DPBS/0.5% Triton X-100 for 5 min at room temperature, further treated with 1% of sodium dodecyl sulfate (SDS) in DPBS for 5 minutes to perform the antigen retrieval, and subsequently washed with DPBS. Then, samples were blocked by DPBS/1% bovine serum albumin (BSA)/10% goat serum for 30 min. Incubation with primary antibodies, with dilution 1:50 (Runx2), 1:100, (COLL I) and 1:200 (OCN) in

DPBS/ 1% bovine serum BSA /10% goat serum, was performed for 5 h at room temperature. Further, samples were washed with DPBS/0.05% Tween 20 surfactant and incubated with Bodipy FL Dye (Fisher) dilution 1:400 to stain the cytoskeleton and secondary antibody anti-mouse conjugated with alexa 555 for 1 h at room temperature. Incubation with secondary antibodies was not performed for Runx2, because primary antibody is labelled FITC. Finally, samples were mounted with Vectashield DAPI for nuclei staining. Detection of protein markers was performed by confocal fluorescence microscope (Zeiss LSM 780, Axio Observer).

The staining antibodies on control materials were performed on whole sample. After washing second antibodies, control materials were fixed and included in cryoprotective medium at -80 °C. Then, samples were cut into slices with 50 μm of thickness and mounted with Vectashield DAPI.

2.9. Histological Analysis

Cultured samples were fixed with formaldehyde, included in optimum cutting temperature compound (OCT), frozen at -80 °C and cut into slices with 17 μm of thickness. Detection of phosphate deposits on Cht/HAp hydrogels were determined using von Kossa staining. Samples were washed with distilled water and incubated in a 5% $AgNO_3$ solution (Sigma-Aldrich) under ultraviolet light for 20 min. Further, samples were washed with distilled water and 2% $Na_2S_2O_3$ (Sigma-Aldrich) to remove unreacted $AgNO_3$. Finally, the cells were stained using a neutral red solution (Sigma-Aldrich) for 2 minutes. Detection of calcium deposits was determined using Alizarin red S staining. Samples were incubated with 2% of alizarin red solution (pH of 4.2; Sigma-Aldrich) for 4 minutes. After staining, samples were washed with distilled water and mounted with 80% of glycerol solution (Sigma-Aldrich).

### 2.10. Statistical analysis

All experiments were performed in triplicates or more. Statistical comparison between two groups was tested using one-way ANOVA test with value $p < 0.05$ and $p < 0.01$ considered statistically significant.

## 3. Results

### 3.1. *In vitro* degradation testing

In the present study, enzymatic degradation of Cht/HAp hydrogel was studied at 37 °C as a function of time, for 28 days, by monitoring swelling behaviour, dry weight loss, molecular weight ($M_w$) and polydispersity index (*PDI*). To distinguish between enzymatic degradation and dissolution, Cht/HAp hydrogels were exposed to phosphate buffer solution (PBS) without and with (1.5 and 500 µg/mL) lysozyme, as used in reported studies (Jin et al., 2009; Moura, Faneca, Lima, Gil & Figueiredo, 2011; Yang et al., 2010). The lysozyme concentration of 500 µg/mL better mimics the *in vivo* physiological conditions, as the lysozyme level in the extracellular matrix of human tissues can increase up to 1,000- fold (Hou et al., 2012) the amount usually found in serum (0.95~2.45 µg/mL) (Jin et al., 2009; Park, Choi & Lee, 2013;).

The results shown in Fig. 1a suggest an increase in swelling ratio with incubation time for all investigated systems. However, there is no significant difference in swelling ratios among 3, 14 and 28 days for Cht/HAp hydrogels (Fig. 1a) incubated in non-enzymatic conditions (Cht/HAp_PBS) and in 1.5 µg/mL of lysozyme solution (Cht/HAp_1.5 µg/mL). For Cht/HAp hydrogel incubated in the 500 µg/mL of lysozyme solution (Cht/HAp_500µg/mL) there is a significant difference between swelling ratios between 3 and 28 days. As seen from Figure 1b the weight loss of Cht/HAp hydrogel in different incubation media follows the decreasing

trend: PBS < 1.5 µg/mL of lysozyme solution < 500 µg/mL of lysozyme solution. However, there is no significant difference in dry weight remaining ratio among 3, 14 and 28 days. Weight average molecular weight ($M_{w)}$ reduction during incubation was observed in all investigated systems (Fig. 1c), and the degradation is the most pronounced in 500 µg/mL of lysozyme solution. Initial molecular weight, $M_{w0} \approx$ 222 000, decreased after 3 and 28 days, in non-enzymatic condition to 170 000 and 113 000, respectively, in 1.5 µg/mL of lysozyme solution to 123 000 and 79 000, respectively, and in 500 µg/mL of lysozyme solution to 48 000 and 36 500, respectively. Polydispersity index stayed around 2 throughout all degradation process which could indicate a random depolymerisation (Holme, Davidsen, Kristiansen & Smidsrød, 2008).

In all investigated systems the decrease in molecular weight is accompanied by an increase of the swelling ratio, but only in system Cht/HAp_500µg/mL a significant difference in swelling ratio between 3 and 28 days was observed. It is expected that shorter chitosan chains in Cht/HAp_500µg/mL, show smaller extent of chain entanglements and physical crosslinking density, compared to other two investigated systems, resulting in higher swelling ratios. To provide a better understanding of the correlation between chitosan molecular weight and swelling ratio other molecular parameters that describe the network structure of hydrogels should be determined, such as the critical entanglement molecular weight and the average molecular weight between crosslinks. (i.e., mesh size).

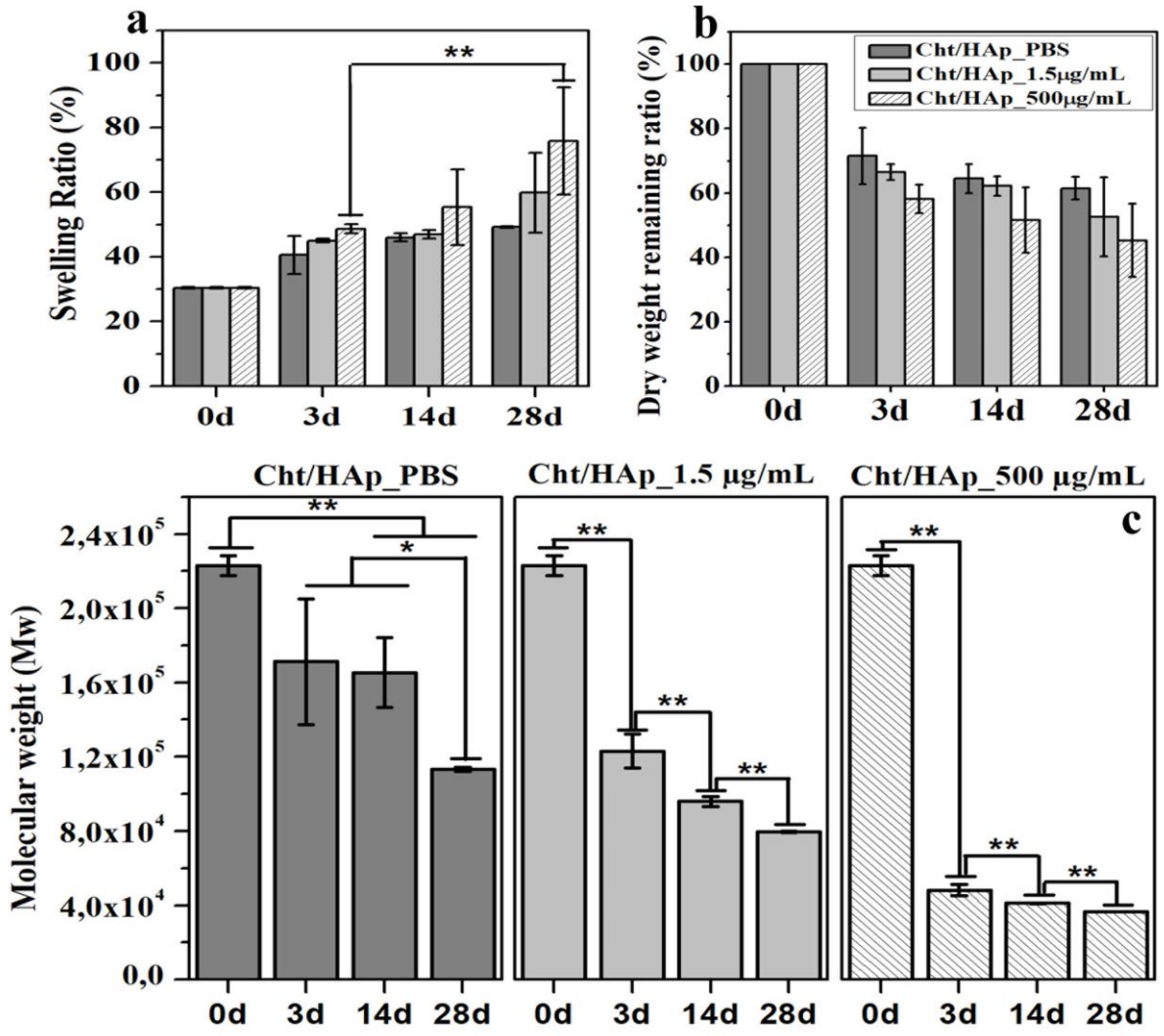


Fig. 1. Swelling ratio (a); dry weight remaining ratio (b); and weight average molecular weight (c) of Cht/HAp hydrogel incubated in different degradation media at 37 °C as a function of time. Significant difference between two groups: *($p < 0.05$), ** ($p < 0.01$).

The microstructures of the cross section of Cht/HAp_PBS and Cht/HAp_1.5 μg/mL hydrogels shown in Fig. 2b confirm larger pores after 3 days of incubation at 37 °C compared to initial Cht/HAp hydrogel (0 day), as a result of water absorption. The pore structure of Cht/HAp_500μg/mL hydrogel is fully disrupted after 3 days of incubation as a result of high degradation rate. However, it retained the porous structure which is important for the diffusion of nutrients, metabolic waste products, and oxygen. In this study, deacetylation degree of chitosan is in the range 0.95 – 0.98 and a high stability under enzymatic conditions

was expected (Freier, Koh, Kazazian & Shoichet, 2005). After 28 days of incubation highly porous structure was maintained in all degradation conditions indicating a stable Cht/HAp hydrogel. SEM micrographs of Cht/HAp hydrogels cross section confirmed uniform degradation through entire volume of hydrogel and good particles distribution of *in situ* precipitated HAp within chitosan matrix (see Fig. 2a). In comparison to the hydrogel prepared by mixing previously prepared hydroxyapatite particles within chitosan/β-glycerophosphate (Chen et al., 2016) *in situ* precipitation performed in this work results in smaller particles size.

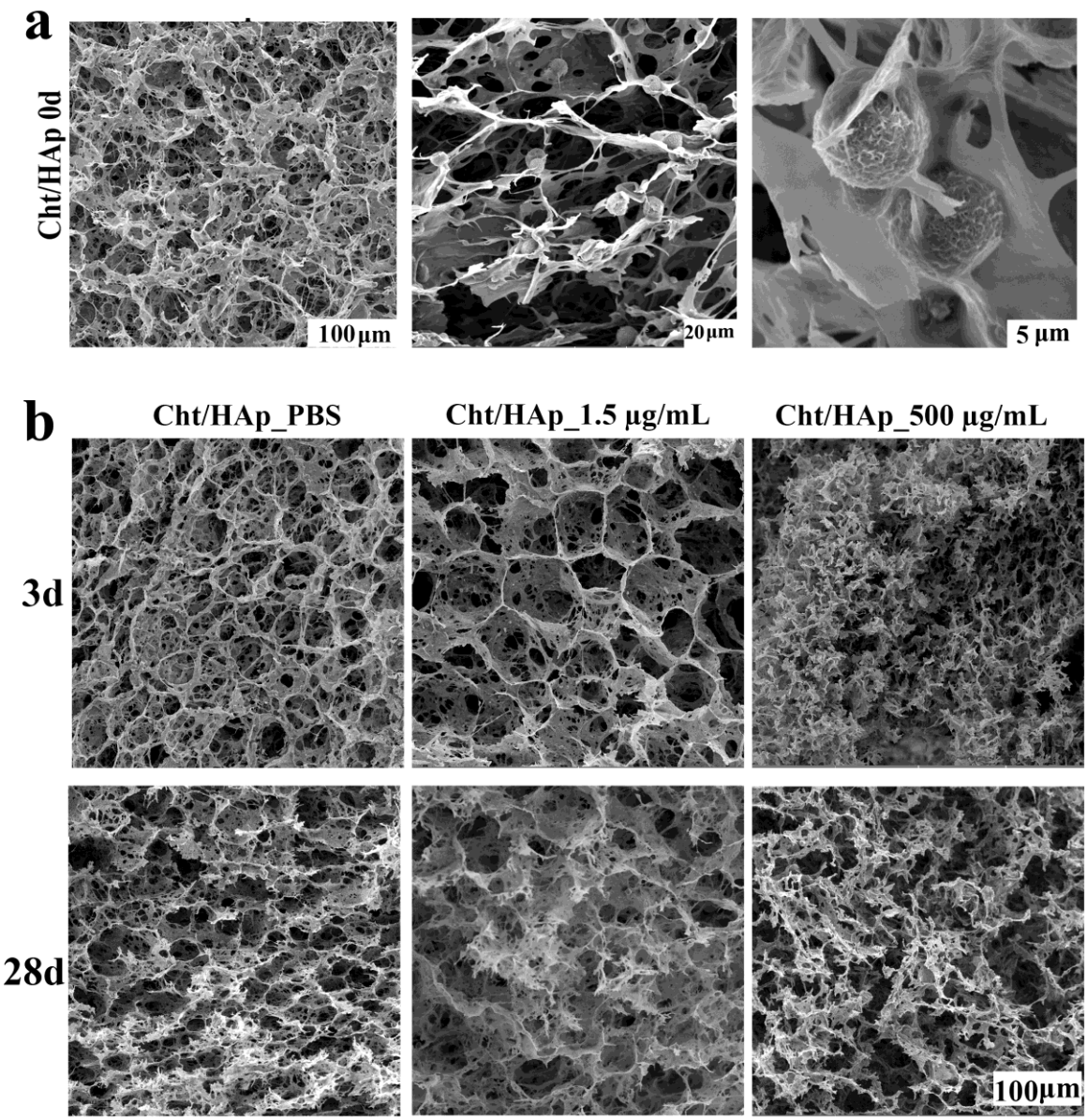

Fig. 2. SEM micrographs of dried hydrogel with *in situ* precipitated HAp particles within chitosan matrix (a) and Cht/HAp hydrogel incubated for 3 and 28 days under different degradation conditions (b).

### 3.2. Biological characterization

As described in experimental section, for both, the hydrogel and the scaffold, the cell counting was performed by imaging three DAPI stained 50 μm slices, of five different replicas. Images were taken by confocal fluorescence microscope in 16-tile mode scanning. Fig 3a represents the average cell number of the total 16 tiles at 3 different slices. It is noteworthy that counted cell number does not represent total cell number, but average number of cells on material slices imaged in 16-tile mode.

As shown in Fig. 3a, lower cell number on scaffold at day 0, compared to hydrogel was observed, although, the same number of cells were encapsulated in the hydrogel and seeded on the scaffold. It could indicate that all cells did not succeed to achieve a stable adhesion and could easily detach from the scaffold. An increase in the number of cells after 7 days of culture was obtained in both Cht/HAp hydrogel and the control, indicating that new injectable Cht/HAp hydrogel is suitable for cell encapsulation and proliferation and can be used as a cell carrier for bone tissue engineering. After an initial increase in cell number, there is not a significant difference in the average cell number between 7 and 14 days. This could indicate that cells stopped proliferating and probably started to differentiate, what was confirmed by the presence of osteogenic markers, as will be shown below. Figure S1 of Supplementary material confirms that cells stayed homogeneously dispersed inside hydrogel during 14 days of cell culture indicating that the microstructure and physically crosslinked chitosan chains do not allow cell to migrate outside the hydrogel.

Cells secrete alkaline phosphatase, a characteristic parameter of osteoblasts. Although there is no significant difference in ALP concentration (Fig. 3b) between 7 and 14 days of cell culture in the Cht/HAp hydrogel, it seems that the tendency is to increase with the culture time. A clear significant increase of ALP secretion was measured in the control scaffolds.

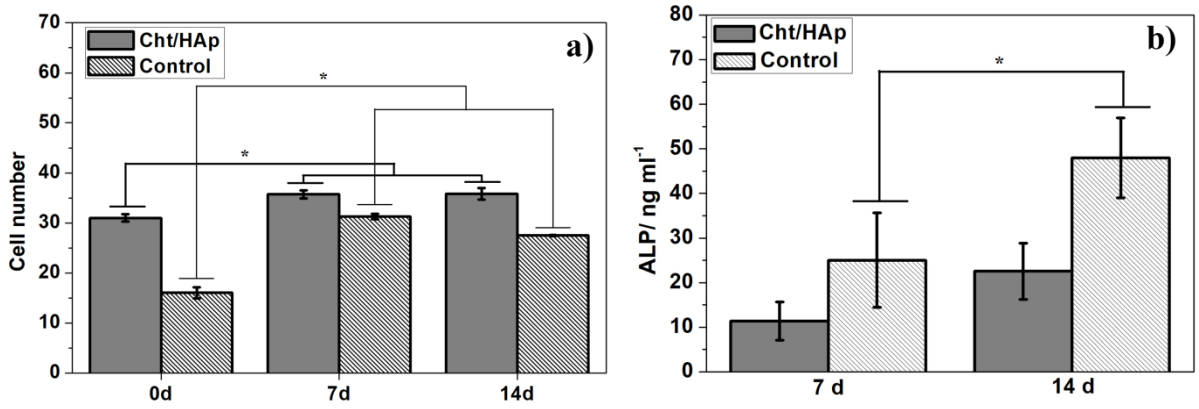


Fig. 3. The cell number (a) and alkaline phosphatase activity (ALP) (b) of MSCs encapsulated in Cht/HAp hydrogel and control after 7 and 14 days of cell culture. Significant difference between two groups ($p$ <0.05) is designated with (*).

Along with ALP activity quantification, osteogenic differentiation of MSC cells encapsulated in Cht/HAp hydrogel was determined by analysing the expression of runt-related transcription factor 2 (Runx2), collagen I (COLL I) and osteocalcin (OCN) at 7 and 14 days of cell culture. Images obtained by confocal fluorescence microscopy are shown in Fig. 4a-c. Cell nuclei stained with DAPI appeared in blue, while Runx2 (Fig. 4a) appeared in green, COLL I (Fig. 4b) and OCN (Fig. 4c) appeared in red and cytoskeleton (actin) in green. Unfortunately, the quality of immunofluorescence images is poor due to strong auto-fluorescence of hydrogel/scaffold. To minimize the sample interference the images were processed by ImageJ software, which resulted in darkening of the final image. To compensate this we completed the study with additional colorimetric stains (alizarin red and von Kossa) as will be shown later.

Previous *in vitro* studies (Komori, 2003) demonstrated that Runx2 can enhance the expression of bone matrix genes like collagen type I, osteopontin, osteocalcin, bone sialoprotein (BSP) and fibronectin. According to that, expression of COLL I and OCN was expected and found at 7 and 14 days of cell culture, implying good osteogenic potential of prepared Cht/HAp hydrogel. The round shape morphology of MSCs is evident after 7 and 14 days of cell culture, which is consistent with the literature (Wang, Rao & Stegemann, 2013; Caliari, Vega, Kwon, Soulas & Burdick, 2016).

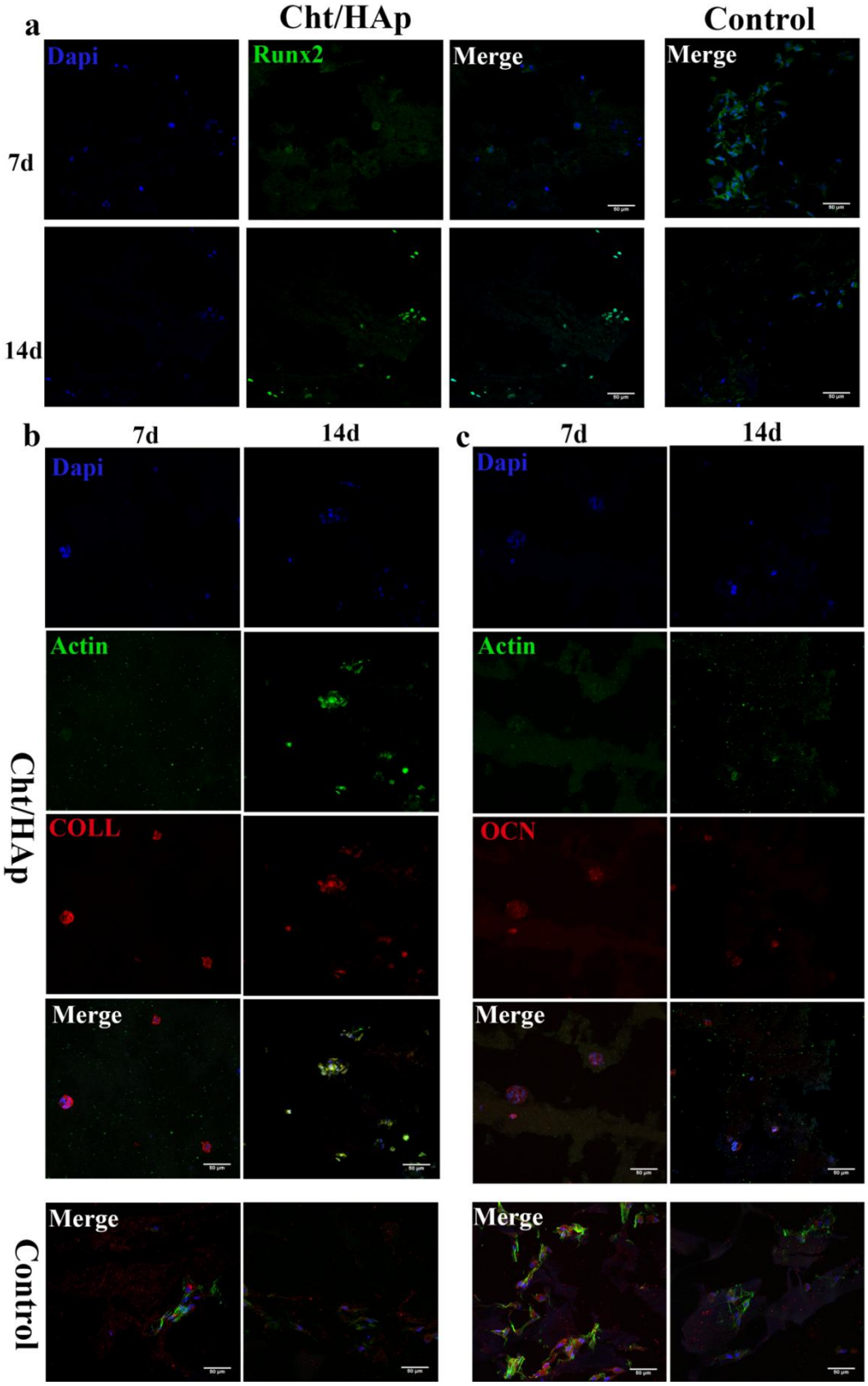


Fig. 4. The expression of Runx2 (a), collagen type I (COLL I) (b) and osteocalcin (OCN) (c) encapsulated in Cht/HAp hydrogels after 7 and 14 days of cell culture. Cell nucleus stained with Dapi (blue fluorescence), Runx2 (green fluorescence) (a). Actin cytoskeleton stained

with phallacidin (green fluorescence), COLL I and OCN (red fluorescence) (b and c). Scale bar: 50 µm.

Mineralized ECM in the Cht/HAp hydrogels was identified by von Kossa and Alizarin red staining (Fig. 5), where calcium deposits are positively stained in red and phosphate deposits in brown or black. After 7 and 14 days of culture higher intensity of red and brown (black) deposits indicate that mineralization of ECM occurred. Obtained results of differentiated cells after 7 and 14 days of cell culture were compared with Cht/HAp hydrogel with undifferentiated cells at day 0 (Ctrl in Fig. 5).

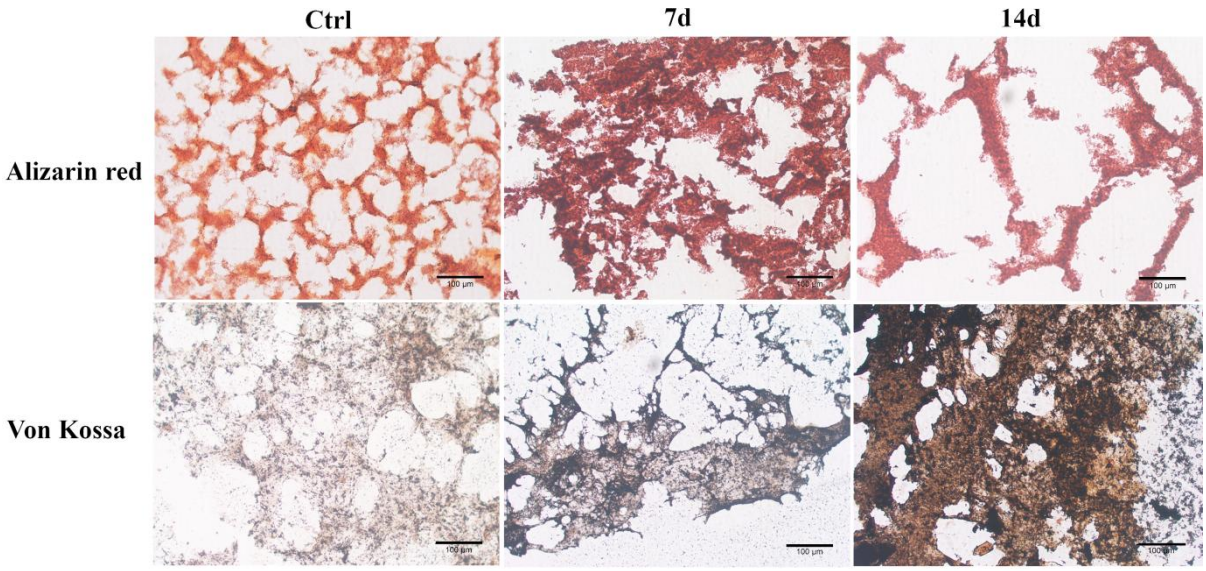


Fig. 5. Positive staining for calcium deposits after 7 and 14 days of culture is observable by red colour determined using alizarin red S assay. Positive staining for phosphate deposits after 7 and 14 days is observable by brown and black colour determined using von Kossa assay. Cht/HAp hydrogel with undifferentiated cells was used to indicate the material/cell interference (Ctrl). Scale bar: 100 µm.

## 4. Discussion

In our previous study (Rogina et al., 2017b) an injectable, pH-responsible, physically crosslinked hydrogel based on chitosan and *in situ* formed hydroxyapatite, with 30% (w/w) of HAp phase, was prepared. The viscoelastic behaviour of hydrogel was observed in the range of strain deformation up to approximately 10%. The G"/G' ratio of 0.04 and linear viscoelasticity above 5% of strain deformation, indicated that chitosan/HAp hydrogel could behave as a strong physical gel. Compared to the storage modulus of similar physically crosslinked chitosan-based system, with 30% (w/w) of bioglass nanoparticles, and *β*-glycerophosphate as a gelling agent (Couto, Hong & Mano, 2009) our gel showed 1.5-fold higher storage modulus, indicating better resistance to shear. Distribution and viability of encapsulated mouse embryonic fibroblasts within the hydrogel up to 7 days of culture was confirmed by *live dead* staining.

As a continuation of previous study, in this work an extensive *in vitro* characterization of the hydrogel, using porcine MSCs, was performed, including, *in vitro* enzymatic degradation during 28 days of incubation, in simulated physiological condiditons. It was hypothesized that *in situ* synthesis of hydroxyapatite within chitosan matrix would provide a homogeneous dispersion of hydroxyapatite particles with positive influence on osteoinduction and differentiation of MSCs that can lead to homogeneous bone regeneration.

Swelling behaviour, structural integrity and rate of degradation are critical variables in hydrogel design that affect the rate of tissue formation. Hydrogels derived from natural polymers often are not stable at physiological conditions and undergo rapid degradation (Tan & Marra, 2010). As cell carriers, hydrogels stability during cell encapsulation and differentiation at physiological conditions is required. Chitosan has the ability to readily swell up when exposed in a biological environment. Degradation of chitosan takes place via hydrolysis, as interactions with water molecules break the polymeric network into smaller chains whereby the β-1-4 N-acetyl glucosamine units of Cht undergo chain scission mainly by

lysozymes present in the body. This phenomenon leads to release of amino sugars, which can be incorporated into metabolic pathways or excreted through the body (Liu, Zhou & Sun, 2012; Qasim et al., 2017; Ren, Yi, Wang & Ma, 2005; Tomihata & Ikada, 1997). Other by products of Cht degradation include saccharides which become part of the normal metabolic process (Kumar, Muzzarelli, Muzzarelli, Sashiwa & Domb, 2004).

The results obtained in this work show that new physically crosslinked Cht/HAp hydrogel is highly stable during 28 days, even in extreme conditions with much higher concentration of lysozyme than physiological, which is important for the eventual future clinical application of the material. The weight loss after 28 days of incubation is comparable to the literature data reported for chemically crosslinked hydrogels based on chitosan, showing 30 – 70 % weight loss after 28 days of incubation under enzymatic physiological conditions, depending on crosslinking degree (Moura et al., 2011; Xu et al., 2016). The big advantage of the synthesis applied in present work is simple chitosan gel formation, feasible under mild conditions, without using toxic cross-linking agents. The cross-sectional SEM images of the freeze-dried hydrogels (Fig. 2) demonstrate a porous and netlike structure and good particles distribution of *in situ* precipitated HAp within chitosan matrix. The porous structures provide an environment suitable for the attachment, growth, and differentiation of MSCs, and transport of nutrients to the cells.

Many *in vitro* and *in vivo* studies have suggested that MSCs have the potential to enhance osteogenesis while being delivered in critical sized bone defects with ability to migrate to defect sites. Despite MSCs capacity to differentiate to osteoblasts, MSCs ability to support a regenerative microenvironment is of great importance. MSCs can differentiate to multiple cell types like chondrocytes, osteoblasts and adipocytes (Oryan, Kamali, Moshiri & Baghaban Eslaminejad, 2017). MSCs were encapsulated in an injectable thermosensitive chitosan-glycerophosphate where differentiation occurred to chondrocytes (Richardson, Hughes, Hunt,

449 Freemont & Hoyland, 2008). The same tendency was observed in other chitosan based
450 hydrogels (Cho et al., 2004; Jin, 2009; Hu, 2012). Wang and Stegemann (Wang &
451 Stegemann, 2010) used β-glycerophosphate as gelling agent to obtain physically crosslinked
452 chitosan hydrogel. High concentration of β-glycerophosphate was required to obtain gelation
453 time below 10 min. Additionally, DNA content of encapsulated human bone marrow
454 mesenchymal stem cells decreased over time suggesting that cells were dying in chitosan
455 hydrogel. Incorporation of previously prepared HAp particles into chitosan/gelatin scaffold
456 enhanced osteogenic differentiation (Zhao, Grayson, Ma, Bunnell & Lu, 2006). In the present
457 work the differentiation of MSCs encapsulated in the Cht/HAp hydrogel was evaluated after 7
458 and 14 days of cell culture. Colorimetric quantification of alkaline phosphatase activity and
459 immunofluorescent imaging was used to detect the expression of osteogenic markers.

460 Detection of Runx2 as a principal osteogenic master gene for bone formation as well as
461 COLL I and OCN, characteristic genes of differentiation process, indicates good osteogenic
462 signal of Cht/HAp hydrogel where MSCs differentiated into an osteoblast phenotype
463 indicating possible application of Cht/HAp hydrogel as cell carrier for bone tissue
464 engineering.

465 Osteogenesis depends on the material's composition, surface properties, charge and
466 wettability, but also on the material stiffness. Literature reports that stiffness of about 1,5 kPa
467 upregulated osteogenic expression whereas softer matrices are not so osteogenic (Murphy,
468 Matsiko, Haugh, Gleeson & O'Brien, 2012). That is the possible reason why the injectable
469 Cht/HAp hydrogel that possess a lower modulus, around 100 Pa (Rogina et.al. 2017b) than
470 the Cht/HAp scaffold has a lower ALP activity compared to the scaffold.

471 The deposition of late osteogenic markers (calcium phosphates) detected by Alizarin red and
472 Von Kossa staining indicated an extracellular matrix (ECM) mineralization. It can be

concluded that Cht/HAp hydrogel provide suitable environment for enhanced osteogenesis of MSCs. Further *in vivo* studies on animal model need to be performed to examine biodegradation and osteogenesis to confirm the applicability of Cht/HAp hydrogel for bone tissue engineering.

## 5. Conclusion

Present research has shown that novel chitosan/hydroxyapatite physically crosslinked hydrogel act as the three-dimensional support for MSCs proliferation and differentiation into osteoblast cells. The expression of characteristic bone genes, Runx2, ALP, COLL I, OCN and calcium phosphate deposits, indicated that ECM mineralisation took place during 14 days of cell culture. MSCs are homogeneously dispersed through entire Cht/HAp hydrogel during cell culture, which is crucial for full bone healing. Prepared Cht/HAp hydrogel is highly stable under physiological and enzymatic conditions supporting the osteogenesis of encapsulated mesenchymal stem cells.

**Acknowledgements**

This work has been supported in part by the Croatian Science Foundation under the project IP-2014-09-3752 by the Spanish Ministry through the MAT2016-76039-C4-1-R project (including the FEDER financial support). The authors want to thank Laura Teruel Biosca from Centre for Biomaterials and Tissue Engineering, Universitat Politècnica de València, for helping with gel permeation chromatography measurements. Joaquin Ródenas-Rochina acknowledges funding by the Consellería de Educación, Investigación, Cultura y Deporte (Generalitat Valenciana) and co-funding by Fondo Social Europeo (FSE) through APOSTD grant (APOSTD/2016/006).

**References**

496 Caliari, S. R., Vega, S. L., Kwon, M., Soulas, E. M., & Burdick, J. A. (2016). Dimensionality
497 and spreading influence MSC YAP/TAZ signaling in hydrogel environments. *Biomaterials*,
498 *103*, 314–323.

499 Chen, Y., Zhang, F., Fu, Q., Liu, Y., Wang, Z., & Qi, N. (2016). In vitro proliferation and
500 osteogenic differentiation of human dental pulp stem cells in injectable thermo-sensitive
501 chitosan/b-glycerophosphate/hydroxyapatite hydrogel. *Journal of Biomaterials Applications*,
502 *31*, 317–327.

503 Chenite, A., Buschmann, M., Wang, D., Chaput, C., & Kandani, N. (2001). Rheological
504 characterisation of thermogelling chitosan/glycerol-phosphate solutions. *Carbohydrate*
505 *Polymers*, *46*, 39–47.

506 Cho, J. H., Kim, S. H., Park, K. D., Jung, M. C., Yang, W. I., Han, S. W., Noh, J. Y., & Lee,
507 J. W. (2004). Chondrogenic differentiation of human mesenchymal stem cells using a
508 thermosensitive poly(N-isopropylacrylamide) and water-soluble chitosan copolymer.
509 *Biomaterials*, *25*, 5743–5751.

510 Couto, D. S., Hong, Z., & Mano, J. F. (2009). Development of bioactive and biodegradable
511 chitosan-based injectable systems containing bioactive glass nanoparticles. *Acta*
512 *Biomaterialia*, *5*, 115–123.

513 Dang, J. M., Sun, D. D., Shin-Ya, Y., Sieber, A. N., Kostuik, J. P., & Leong, K. W. (2006).
514 Temperature-responsive hydroxybutyl chitosan for the culture of mesenchymal stem cells and
515 intervertebral disk cells. *Biomaterials*, *27*, 406–418.

516 Debnath, T., Ghosh, S., Potlapuvu. U. S., Kona, L., Kamaraju, S. R., Sarkar, S., Gaddam, S.,
517 & Chelluri, L. K. (2015). Proliferation and Differentiation Potential of Human Adipose-

518 Derived Stem Cells Grown on Chitosan Hydrogel. *PLOS ONE, 10*, Article Number:
519 e0120803.

520 Demirtaş, T. T., Irmak, G., & Gümüşderelioğlu, M. (2017). A bioprintable form of chitosan
521 hydrogel for bone tissue engineering. *Biofabrication, 9*, Article number:035003.

522 Freier, T., Koh, H. S., Kazazian, K., & Shoichet, M. S. (2005). Controlling cell adhesion and
523 degradation of chitosan films by N-acetylation. *Biomaterials, 26*, 5872–5878.

524 Frohbergh, M. E., Katsman, A., Botta, G. P., Lazarovici, P., Schauer, C. L., Wegst, U. G. K.,
525 & Lelkes, P. I. (2012). Electrospun hydroxyapatite-containing chitosan nanofibers crosslinked
526 with genipin for bone tissue engineering. *Biomaterials, 33*, 9167–9178.

527 Gámiz-González, M. A., Guldris, P., Antolinos Turpín, C. M., Ródenas Rochina, J., Vidaurre,
528 A., & Gómez Ribelles, J. L. (2017). Fast degrading polymer networks based on
529 carboxymethyl chitosan, *Materials Today Communications, 10*, 54–66.

530 Holme, H. K., Davidsen, L., Kristiansen, A., & Smidsrød, O. (2008). Kinetics and
531 mechanisms of depolymerization of alginate and chitosan in aqueous solution. *Carbohydrate*
532 *Polymers, 73*, 656–664.

533 Hou, Y. P., Hu, J. L., Park, H., & Lee, M. (2012). Chitosan-based nanoparticles as a sustained
534 protein release carrier for tissue engineering applications. *Journal of Biomedical Materials*
535 *Research A, 100*, 939–944.

536 Hu, J., Hou, Y., Park, H., Choi, B., Hou, S., Chung, A., & Lee, M. (2012). Visible light
537 crosslinkable chitosan hydrogels for tissue engineering. *Acta Biomaterialia, 8*, 1730–1738.

538 Jin, R., Moreira Teixeira, L. S., Dijkstra, P. J., Karperien, M., van Blitterswijk, C. A., Zhong,
539 Z. Y., & Feijen, J. (2009). Injectable chitosan-based hydrogels for cartilage tissue
540 engineering. *Biomaterials, 30*, 2544–2551.

Komori, T. (2003). Requisite roles of Runx2 and Cbfb in skeletal development. *Journal of Bone and Mineral Metabolism, 21,* 193–197.

Kumar, M. N. V. R., Muzzarelli, R. A. A., Muzzarelli, C., Sashiwa, H., & Domb, A. J. (2004). Chitosan chemistry and pharmaceutical perspectives. *Chemical Reviews, 104,* 6017–6084.

Lennon, D. P., & Caplan Al. (2006). Isolation of human marrow-derived mesenchymal stem cells. *Experimental Hematology, 34,* 1604–1605.

Liu, H., Peng, H., Wu, Y., Zhang, C., Cai, Y., Xu, G., Li, Q., Chen, X., Ji, J., Zhang, Y., OuYang, H. W. (2013). The promotion of bone regeneration by nanofibrous hydroxyapatite/chitosan scaffolds by effects on integrin-BMP/Smad signaling pathway in BMSCs. *Biomaterials, 34,* 4404–4417.

Liu, M., Zeng, X., Ma, C., Yi., H., Ali, Z., Mou, X., Li, S., Deng, Y., & He, N. (2017). Injectable hydrogels for cartilage and bone tissue engineering. *Bone Research, 5,* Article Number: 17014.

Liu, Y., Zhou, C., & Sun, Y. (2012). A biomimetic strategy for controllable degradation of chitosan scaffolds. *Journal of Materials Research, 27,* 1859–1868.

Moura, M. J., Faneca, H., Lima, M .P., Gil, M. H., & Figueiredo, M. M. (2011). In Situ Forming Chitosan Hydrogels Prepared via Ionic/Covalent Co-Cross-Linking. *Biomacromolecules, 12,* 3275–3284.

Murphy, C. M., Matsiko, A., Haugh, M. G., Gleeson, J. P., & O'Brien, F. J. (2012). Mesenchymal stem cell fate is regulated by the composition and mechanical properties of collagen-glycosaminoglycan scaffolds. *Journal of the Mechanical Behavior of Biomedical Materials, 11,* 53–62.

564 Naderi-Meshkin, H., Andreas, K., Matin, M. M., Sittinger, M., Bidkhori, H. R., Ahmadiankia,
565 N., Bahrami, A. R., & Ringe, J. (2014). Chitosan-based injectable hydrogel as a promising in
566 situ forming scaffold for cartilage tissue engineering. *Cell Biology International*, *38*, 72–84.

567 Oryan, A., Kamali, A., Moshiri, A., & Baghaban Eslaminejad, M. (2017). Role of
568 Mesenchymal Stem Cells in Bone Regenerative Medicine: What Is the Evidence?. *Cells*
569 *Tissues Organs*, *204*, 59–83.

570 Park, H., Choi, B., Hu, J., & Lee, M. (2013). Injectable chitosan hyaluronic acid hydrogels for
571 cartilage tissue engineering. *Acta Biomaterialia*, *9*, 4779–4786.

572 Peter, M., Ganesh, N., Selvamurugan, N., Nair, S. V., Furuike, T., Tamura, H., & Jayakumar,
573 R. (2010). Preparation and characterization of chitosan-gelatin/nanohydroxyapatite composite
574 scaffolds for tissue engineering applications. *Carbohydrate Polymers*, *80*, 687–694.

575 Porstmann, B., Jung, K., Schmechta, H., Evers, U., Pergande, M., Porstmann, T., Kramm, H.
576 J., & Krause, H. (1989). Measurement of lysozyme in human body fluids: comparison of
577 various enzyme immunoassay techniques and their diagnostic application. *Clinical*
578 *Biochemistry*, *22*, 349–355.

579 Qasim, S. B., Husain, S. , Huang, Y., Pogorielov, M., Deineka, V., Lyndin, M, Rawlinson, A.,
580 & Rahman, I. U. (2017). In-*vitro* and in-*vivo* degradation studies of freeze gelated porous
581 chitosan composite scaffolds for tissue engineering applications. *Polymer Degradation and*
582 *Stability*, *136*, 31–38.

583 Racine L., Texier, I., & Auzély-Velty, R. (2017). Chitosan-based hydrogels: recent design
584 concepts to tailor properties and functions. *Polymer International*, *66*, 981–998.

585 Ren, D., Yi, H., Wang, W., & Ma, X. (2005). The enzymatic degradation and swelling
586 properties of chitosan matrices with different degrees of N-acetylation. *Carbohydrate*
587 *research, 340,* 2403–2410.
588 Richardson, S. M., Hughes, N., Hunt, J. A., Freemont, A. J., & Hoyland, J. A. (2008). Human
589 mesenchymal stem cell differentiation to NP-like cells in chitosan–glycerophosphate
590 hydrogels. *Biomaterials, 29,* 85–93.

591 Rodenas-Rochina, J., Kelly, D. J., Ribelles, J. L. G., & Lebourg, M. (2016). Compositional
592 changes to synthetic biodegradable scaffolds modulate the influence of hydrostatic pressure
593 on chondrogenesis of mesenchymal stem cells. *Biomedical Physics & Engineering Express, 2,*
594 Article Number: 035005.

595 Rogina, A., Antunović, M., Pribolšan, L., Caput Mihalić, K., Vukasović, A., Ivković, A.,
596 Marijanović, I., Gallego Ferrer, G., Ivanković, M., & Ivanković, H. (2017a). Human
597 mesenchymal stem cells differentiation regulated by hydroxyapatite content within chitosan-
598 based scaffolds under perfusion conditions. *Polymers, 9,* 387–404.

599 Rogina, A., Ressler, A., Matić, I., Gallego Ferrer, G., Marijanović, I., Ivanković, M., &
600 Ivanković H. (2017b). Cellular hydrogels based on pH-responsive chitosan-hydroxyapatite
601 system. *Carbohydrate Polymers, 166,* 173–182.

602 Rogina, A., Rico, P., Gallego Ferrer, G., Ivanković, M. & Ivanković, H. (2015). Effect of in
603 situ formed hydroxyapatite on microstructure of freeze-gelled chitosan-based biocomposite
604 scaffolds. *European Polymer Journal, 68,* 278–287.

605 Rogina, A., Rico, P., Gallego Ferrer, G., Ivanković, M., & Ivanković, H. (2016). In situ
606 hydroxyapatite content affects the cell differentiation on porous chitosan/hydroxyapatite
607 scaffolds. *Annals of Biomedical Engineering,. 44,* 1107–1119.

608 Sá-Lima H., Caridade, S. G., Mano, J. F., & Reis, R. L. (2010). Stimuli-responsive chitosan-
609 starch injectable hydrogels combined with encapsulated adipose-derived stromal cells for
610 articular cartilage regeneration. *Soft Matter, 6*, 5184–5195.
611 Ta, H. T., Dass, C. R., & Dunstan, D. E. (2008). Injectable chitosan hydrogels for localised
612 cancer therapy. *Journal of Controlled Release, 126*, 205–216.
613 Tan, H., & Marra, K. G. (2010). Injectable, biodegradable hydrogels for tissue engineering
614 applications. *Materials, 3*, 1746–1767.
615 Thorpe, S. D., Buckley, C. T., Vinarfell, T., O'Brien, F. J., Campbell, V. A., & Kelly, D. J.
616 (2008). Dynamic compression can inhibit chondrogenesis of mesenchymal stem cells.
617 *Biochemical and Biophysical Research Communications, 377*, 458–462.
618 Tomihata, K., & Ikada,Y. (1997). In vitro and in vivo degradation of films of chitin and its
619 deacetylated derivatives. *Biomaterials, 18*, 567–575.
620 Wang, L., Rao, R. R., & Stegemann, J. P. (2013). Delivery of Mesenchymal Stem Cells in
621 Chitosan/Collagen Microbeads for Orthopedic Tissue Repair. *Cells Tissues Organs, 197*,
622 333–343.
623 Wang, L., & Stegemann, J. P. (2010). Thermogelling chitosan and collagen composite
624 hydrogels initiated with β-glycerophosphate for bone tissue engineering. *Biomaterials, 31*,
625 3976–3985.
626 Xu, H., Zhang, L., Bao, Y., Yan, X., Yin, Y., Li, Y., Wang, X., Huang, Z., & Xu, P. (2016).
627 Preparation and characterization of injectable chitosan–hyaluronic acid hydrogels for nerve
628 growth factor sustained release. *Journal of Bioactive and Compatible Polymers, 32*, 1–17.

Yang, B., Li, X., Shi, S., Kong, X., Guo, G., Huang, M., Luo, F., Wei, Y., & Zhao, X. (2010). Preparation and characterization of a novel chitosan scaffold. *Carbohydrate Polymers, 80,* 860-865.

Zhao, F., Grayson, W. L., Ma, T., Bunnell, B., & Lu, W. W. (2006). Effects of hydroxyapatite in 3-D chitosan–gelatin polymer network on human mesenchymal stem cell construct development. *Biomaterials, 27,* 1859–1867.

Supplementary data

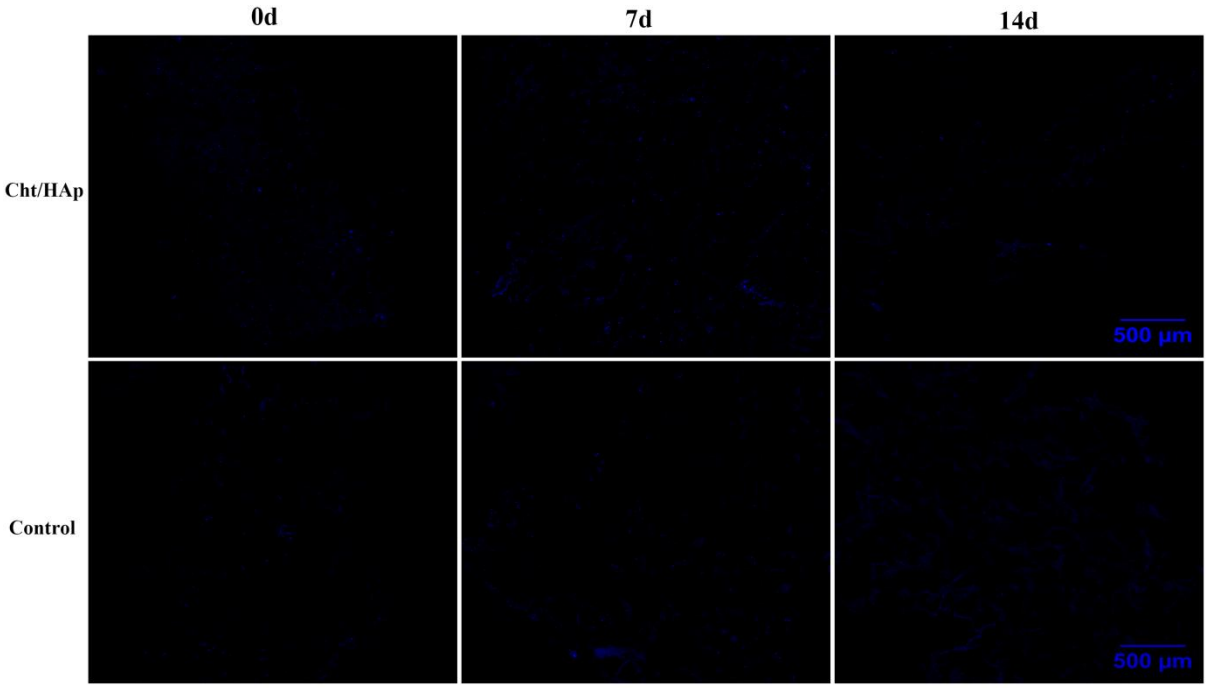


Figure 1. Cell distribution through the cross section of Cht/HAp hydrogel and Control after 0, 7 and 14 days of cell culture (c).

644

645

646

647

648

649